ONE-DIMENSIONAL CALCULATIONS FOR AXIAL PULLBACK FORCE DISTRIBUTIONS IN PIPES DURING DIRECTIONAL DRILLING INSTALLATIONS

A. G. Chehab and I. D. Moore
GeoEngineering Centre at Queen's –RMC, Queen's University, Kingston, Ontario, Canada

ABSTRACT
This paper describes one dimensional modeling to estimate tensile stresses within pipes during pullback. This is achieved by dividing the pipe into elements, simulating the movement of the pulling head, and calculating gravity, friction, and drag forces applied on each element based on its location along the borehole. Estimates of axial force history along the pipe throughout the insertion process are obtained by integrating the elemental forces over the pipe length. The procedure is used to study axial force distributions and cyclic response of pipes during pulling operations where the time history of movement of the pulling head is pre-determined.

RÉSUMÉ
Cet article décrit modeler unidimensionnel pour estimer des efforts de tension dans des pipes pendant le retrait. Ceci est réalisé en divisant la pipe en éléments, en simulant le mouvement de la tête de traction, et en calculant la pesanteur, le frottement, et les forces de résistance à l'avancement appliquées sur chaque élément basé sur son endroit le long du forage. Des évaluations de la force et de l'histoire axiales d'effort le long de la pipe dans tout le procédé d'insertion sont obtenues en intégrant les forces élémentaires au-dessus de la longueur de pipe. Le procédé est employé pour étudier des distributions axiales de force et la réponse cyclique des pipes pendant des extractions où l'histoire de temps du mouvement de la tête de traction est déterminée à partir de l'installation de traction utilisée. Le rendement modelant est comparé aux données fournies par des essais sur le terrain.

1. INTRODUCTION

'*Horizontal directional drilling (HDD) is a technique for installing pipes or utility lines below ground using a surface-monitored drilling rig that launches and places a drill string at a shallow angle to the surface and has tracking and steering capabilities*' (ASTM F 1962-99). The operation involves three main stages:

Pilot Bore excavation:
A pilot hole is first advanced using a drill rig operating from the ground surface. A specially designed tip enables steering of the drill head until it is brought back to the surface at the desired location. To conform to the designed path and avoid hitting other infrastructure, the drill head is usually monitored using a remote sensor.

Back-reaming:
The drill bit is replaced with a back-reamer that is pulled back to enlarge the borehole size up to the desired diameter. Multiple reaming passes may be required depending on the soil type and the required degree of borehole enlargement.

Pull back:
The new pipe is attached to the drill string and pulled back into the borehole. The pulling process is carried out in steps or cycles. In each cycle, the pipe head is pulled by the rig with a fairly constant speed for a specific distance that depends on the rig capacity and the length of the pulling rods. The pulling then stops and time is allowed for removal of each drill rod in turn.

During the pullback operation the pipe is subjected to loading from the drill string as well as shear stresses between the outer surface of the pipe and the surrounding environment (fluidic drag from the drilling mud, static or kinetic friction from the surrounding soil or materials at the ground surface). These loads produce complex axial stress distributions that vary both along the pipe and with time.

After insertion, the pipe is released from the rig and left to recover for a short time period. Finally the pipe is attached to existing infrastructure (such as manholes or hydrants) and placed into service.

Even after installation, tensile stresses continue to vary along the pipe and with time, especially for polymer pipes since viscoelastic strain recovery is prevented once the pipe is attached to its supply and termination points. The axial stresses during insertion and those that occur over the service life of the new pipe may influence the performance of the pipe selected.

2. INSTALLATION LOADS

2.1 Load components

During installation, the pipe interacts with the borehole and the drilling mud. If a straight segment is considered (Figure 1), the main applied forces are due to gravity, friction between the pipe and the ground surface or the borehole wall, and viscous drag from the drilling mud.

2.2 Gravity Forces

The gravity force depends on the pipe weight in case of dry installations and the net buoyant force, i.e. resultant of the pipe weight and the buoyancy force resulting from submerging the pipe in the drilling fluid (mud) in case of wet installations. For inclined segments, the net gravity or buoyancy force component along the pipe axis contributes to the total tensile force applied to the pipe, while the component normal to the pipe axis contributes to the normal force producing friction between the segment and the wall of the borehole.

In dry installations, the pipe segment will rest on the invert of the borehole. In wet installations however, buoyancy forces are usually higher than self weight and the segment is pushed up against the crown of the borehole.

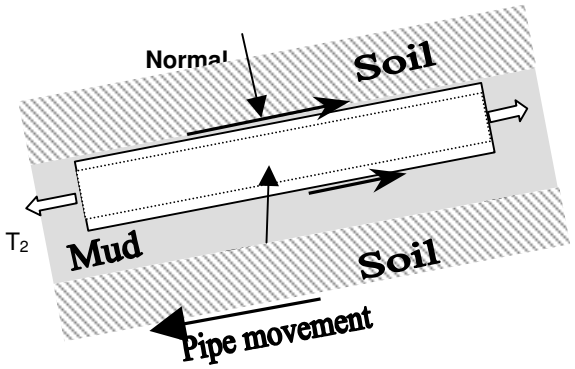

Figure 1. Installation forces on a straight pipe segment

2.3 Frictional forces

Forces also develop due to friction between the pipe and the borehole wall or the ground surface (for segments not yet in the borehole). While gravity forces may act with or against the pipe movement direction, frictional forces always act against the pipe movement.

2.4 Drag forces

Fluid drag is the shear force applied on the outer surface of the pipe being installed as a result of the movement of the viscous drilling mud relative to the pipe being installed. The drilling fluid is usually pumped continuously during the drilling, reaming and pullback processes. Even if no fluid is pumped during the pullback process, any advance of the pipe through the mud confined in the borehole will cause the displaced mud to flow out of bore, i.e. past the pipe and/or the drilling string. That relative movement will still cause some drag forces on the pipe.

Fluid drag depends mainly on the properties of the slurry (drilling fluid containing soil cuttings), the annulus opening geometry and configuration (pipe and borehole size and eccentricity), and the rate of mud flow relative to pipe (pumping rate and rate of pipe advance).

2.5 Curves

2.5.1 Force Components at Curves

Pulling a pipe segment through a curve not only causes bending stresses, but also magnifies the tensile force required to pull the segment. This is due to the additional normal force resulting when the pipe is forced to conform to the curve (due to bending stiffness) as well as the associated friction (the 'capstan' effect, explained below).

2.5.2 Capstan Effect

When a flexible pipe is pulled around a curve, "extra" normal force is created as a result of the change in the direction of the pulling force applied on the curved surface being considered, and friction between that curved surface and the pipe.

2.5.3 Pipe Bending/Stiffness Effect

Bending stresses and additional normal forces develop in the pipe segment when it is forced to conform to a horizontal or vertical curve. The tighter the radius of curvature, the higher the stresses and the normal forces that result. The additional normal forces lead to higher frictional forces and increased pulling forces.

For large diameter steel pipes, bending stresses and additional normal forces can be significant and should be considered. For polyethylene (PE) pipe, the safe curve radii are usually dictated by the drilling rod capacity, since they are stiffer than PE pipes and are subject to cyclic bending stresses as the curved drill string rotates. Research studies indicate that contributions from bending stiffness of PE pipes to increases in pulling force are insignificant over well designed curves. For example, Dareing and Ahlers (1991) analyzed the pullout force needed to remove drill strings from high curvature well bores, and concluded that the weighted cable or string model (that assumes zero flexural stiffness EI) provides a reasonable approximation of the pulling load, provided there are no severe local curves.

3. EXISTING METHODS FOR LOAD CALCULATION

3.1 Introduction to pulling force equations

This section reviews methods currently available for estimating tensile pull loads on pipe installed using horizontal directional drilling (see Baumert and Allouche 2002 for further discussion).

3.2 Driscopipe Method

The Driscopipe Method (Driscopipe, 1993) is considered to be the simplest procedure. The bore path is broken into linear segments. The contribution of each segment to the total pull load is calculated using segment geometry (length L and angle θ). This method neglects the mud drag and load magnification at curves.

3.3 Drillpath Method

The Drillpath Software (Drillpath, 1996) is a three dimensional approach discretizing the pipe into segments that transmit axial forces only (i.e. strings). This neglects the mud drag and the pipe stiffness effect, and relates the load magnification at curves to capstan effect only.

3.4 PRCI Method

The PRCI method (Huey et al, 1996) estimates the maximum pulling load for HDD installations. It assumes that the maximum load occurs toward the end of the pull, and accounts for both mud drag forces and the pipe bending stiffness effect.

3.5 ASTM F 1962 – 99 Method

The American Society for Testing and Materials provides design equations for the estimation of pulling loads applied to the installed pipe at the pipe entry point, the first bend, the second bend, and the pipe exit points.

The ASTM equations are based on assumptions such as:

- The effect of the pipe bending stiffness is neglected.
- The entry and exit points have the same elevation (i.e. the ground surface is horizontal).
- The intermediate span (L2) is horizontal.

3.6 Polak and Lasheen Mechanical Model

Polak and Lasheen (2002) developed a model to calculate the interaction between the pipe and the borehole and the resulting pulling loads. The model accounts for pipe bending stiffness effect and the mud drag. It assumes that all bends in the borehole are sharp with zero radius of curvature, which makes bending of the pipe purely dominated by the oversize ratio (ratio of the borehole diameter to the pipe diameter) and angle of change of direction. The assumption may lead to substantial overestimation of the pulling load magnification at bends, especially for low oversize ratios.

3.7 Empirical Design Table of in-bore resistance

Baumert et al. (2004) proposed a set of tables or empirical design charts to provide estimates of pulling loads in the form of load per unit pulling length. The tables or charts can be generated using a large database of monitored installations in different soil types, borehole profiles, pipe diameters and various construction qualities. This approach provides preliminary design values and assumes linear increase of pulling load with distance.

All the previous approaches treat the installation loads as monotonic (not cyclic), and they are not able to provide information on the cyclic nature of tensile pulling loads, nor the potential effect of soil stiffness on the pipe-soil interaction during installation. Furthermore, they do not provide the pattern of axial force along the pipeline both during and after installation.

4. MODEL DEVELOPMENT

4.1 Model introduction

The model developed in this study is capable of calculating the tensile stress at every point in the pipe being installed at any specific time during the installation process. It considers gravity forces, friction forces (in bore and on the ground surface), mud drag forces, and accounts for the load magnification at curves due to the capstan effect.

The pipe is divided into a number of elements. The location and orientation of each element is determined at the end of each time step and different elemental loads are calculated accordingly.

4.2 Borehole Profile:

The model considers the standard and most common borehole profile that consists of three straight segments and three curves as shown in Figure 2 (though it could readily be extended to consider more complex boring geometries). Lengths L_1, L_2, L_3 provide horizontal positions of the entry, intermediate and exit segments. Angles β_1, β_2 and β_3 define the inclination of the three segments. Values R_1 R_{12} and R_{23} are the radii of curvature of the entry and intermediate curves. In addition, β_o represents the average ground surface inclination at the pipe entry point. No horizontal curves are accounted for in the basic model.

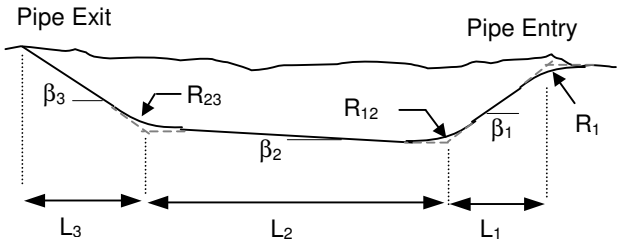

Figure 2. A typical borehole profile.

4.3 Pipe Movement

The movement of every segment of the pipe is associated with the movement of the pulling head, which depends on several factors such as the rig size, pulling speed, length of each pulling rod, and time required to remove pulled rods.

As previously stated, the pulling stage is usually carried out in steps, Figure 3. In each step, the pipe head is pulled with a constant speed for a distance usually equal to the length of a single pulling rod. The pulling then stops for several seconds to remove the drill segment that was recovered.

The movement of the head is represented by a stepped ramp function:

$$\text{Move}(t) = \begin{cases} \text{NPC}.\text{PL} + \left(\frac{\text{PL}}{\text{TP}}\right).(t - \text{NPC} \times (\text{TP} + \text{TR})) & t_c < \text{TP} \\ (\text{NPC}+1).\text{PL} & \text{TP} < t_c < \text{TP} + \text{TR} \end{cases} \quad [1]$$

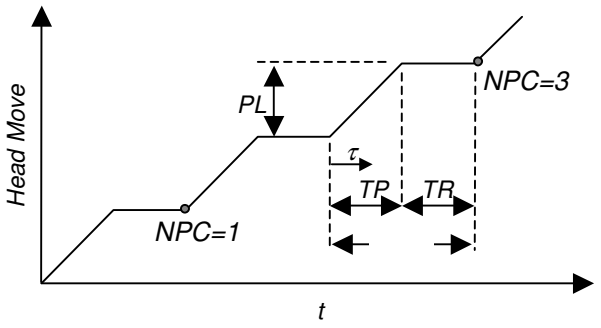

Figure 3. Time history of pipe head movement

Now, PL is the length pulled per cycle, TP and TR are the pulling time and rest time in each cycle, t is the time measured from the beginning of the process, and τ is the time measured from the beginning of each cycle.

4.4 Applied Loads

At any time, the location of each element of the pipe can be determined knowing the location of the pulling head and the location of the element with respect to the pulling head.

Loads applied on each element are calculated knowing its location and the properties of pipe, mud and soil.

The gravity force $\Delta P_{gravity}$ per unit length is given by:

$$\Delta P_{gravity} = \frac{\pi}{4}\left(\gamma_{mud}.OD^2 - \gamma_{pipe}(OD^2 - ID^2)\right).\sin\beta \quad [2]$$

where OD and ID are the external and internal diameters of the pipe, γ is the specific weight, and β is the inclination angle of the element under consideration. The first term in the equation accounts for buoyancy, whereas the second term accounts for the pipe weight. For dry installation where no mud is used, γ_{mud} can be set equal to zero.

Pipe soil interaction leads to shear at the external surface of the pipe, mainly due to friction between the pipe and the borehole wall (μ_{bore}) or ground surface ($\mu_{surface}$). Adhesion may also contribute in some cases. The maximum shear force that can be mobilized per unit length is given by:

$$\text{Max. Shear} = \alpha.A_{cont} + \mu.N \quad [3]$$

where α is the adhesion, A_{cont} is the contact area per unit length, and μ is the coefficient of friction between the pipe and the borehole wall or ground surface. For a straight element, the normal force per unit length N is given by:

$$N = \frac{\pi}{4}\left(\gamma_{mud}.OD^2 - \gamma_{pipe}(OD^2 - ID^2)\right).\cos\beta \quad [4]$$

For a Newtonian fluid with viscosity μ, flowing in a concentric annulus, the drag shear stress τ_p and the mud drag force per unit length are given by:

$$\tau_p = \frac{1}{4}\frac{dp}{dl}\left[\frac{R_{bh}^2 - R_p^2}{R_p \ln(R_{bh}/R_p)} - 2R_p\right] + \frac{\mu V_p}{R_p \ln(R_{bh}/R_p)} \quad [5]$$

$$\Delta P_{drag} = 2\pi R_p.\tau_p \quad [6]$$

where R_{bh} and R_p are the radii of the borehole and pipe respectively, and V_p is the pipe movement velocity. The pressure gradient dp/dl can be solved, if flow rate Q of the drilling mud in the borehole annulus is known:

$$Q = \frac{\pi}{8\mu}\left(\frac{dp}{dl}\right)\left[R_0^4 - R_i^4 - \frac{(R_0^2 - R_i^2)^2}{\ln(R_0/R_i)}\right] + \pi V_p\left[R_p^2 - \frac{R_{bh}^2 - R_p^2}{2\ln(R_{bh}/R_p)}\right] \quad [7]$$

For an eccentric annulus, a modification factor that is a function of eccentricity can be applied to the calculated pressure loss (Haciislamoglu and Langlinas, 1990).

4.5 Forces at Curves:

The change in direction of the pipe is associated with additional normal force N_{curve} that is equal to:

$$N_{curve} \approx T.d\beta \quad [8]$$

where dβ is the change in direction along the element under consideration. To account for the curve effect, N_{curve} is added to N in Equation 3. In addition, all elemental forces are divided by (cos(dβ/2)-μ.cos(dβ/2)).

4.6 Pipe-Soil Interaction:

The interaction between the pipe and the soil (borehole or ground surface) is assumed to exhibit elastoplastic behaviour as shown in Figure 4. The relative movement between the pipe and the surrounding soil is accompanied by linear increase in the interaction shear. This increase continues until the full shear limit given by Equation 3 is mobilized. Further relative displacement takes place as slippage at a constant shear force. Switching the direction of the relative movement will decrease the shear force linearly with a slope equal to K.

The slope K depends on several factors including the soil properties (modulus and Poisson's ratio), soil-mud cake, borehole geometry, borehole depth, and bedrock depth.

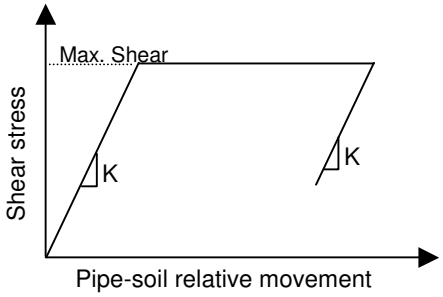

Figure 4. Assumed pipe-soil shear interaction mechanism

4.7 Load Integration:

The contribution of loads on an element n is given by:

$$\Delta T_n = \frac{\Delta P_{gravity} + \Delta P_{shear} + \Delta P_{drag}}{\cos d\beta - \mu . \sin d\beta} \qquad [9]$$

The total tensile force is computed by integrating the loads over all the elements starting with the element at the pipe tail where tension is zero. i.e.

$$T_n = \sum_{i=1}^{n} \Delta T_i \qquad [9]$$

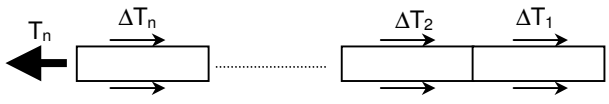

Figure 5. Total load accumulation over pipe length

5. VALIDATION, RESULTS AND DISCUSSIONS

To evaluate the model, calculations are first compared to those from other methods. The model was used to compute the tensile forces along a steel pipe during a horizontal directional drilling installation reported by Baumert et al. (2002).

A 1275 m long crossing to a depth of 50 m of a large diameter (610 mm) steel pipe was chosen (figure 6). The borehole profile consists of three segments, a -10° entry segment, horizontal intermediate segment and a +10° exit segment. Two curves of 750 m radius provide transition between the segments.

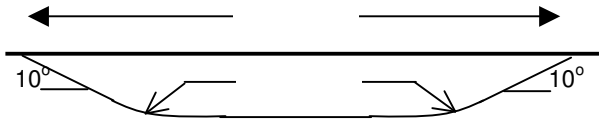

Baumert et al. (2002) used the Driscopipe, Drillpath, and PRCI methods to evaluate the pulling force along the profile for three sets of parameters representing upper bound values, lower bound, and intermediate or average values. The upper and lower bound parameters are given in Table 1.

Table 1. Characteristics of tested soils.

	$\mu_{surface}$	μ_{bore}	γ_{mud} (kN/m³)
Low parameter set	0.0	0.21	10.0
High parameter set	0.5	0.3	14.4

Figures 7a and 7b show the calculations of Baumert et al. (2002) for upper and lower bound parameters, as well as calculations from the new model presented here (assuming zero adhesion). The predictions of the ASTM formulae are also shown. Both adhesion and mud drag are not considered in the calculations.

The predictions of the model developed in this study agree well with those of the Drillpath and PRCI methods. All the methods produce load per unit length in linear segments. The differences are mainly at curves, where the Driscopipe method always predicts lower pulling loads since it does not account for load magnification at curves.

Though the PRCI method accounts for the pipe stiffness effect, it produced values very close to those of the Drillpath method since the curves are well designed with high radius of curvature. At low levels of pulling load, the PRCI predicts slightly higher load magnification at curves. However, the difference decreases as pulling load

increases since the capstan effect becomes the dominant factor. At very high pulling load, the Drillpath method predicts higher load magnification at curves.

The plots in Figure 7 provide general estimates of the pulling loads along the pipe. It is important though to anticipate how the load changes during test times (while rods are being removed), and how that is affected by the stiffness of the pipe and the surrounding soil. For that purpose, another problem is now examined.

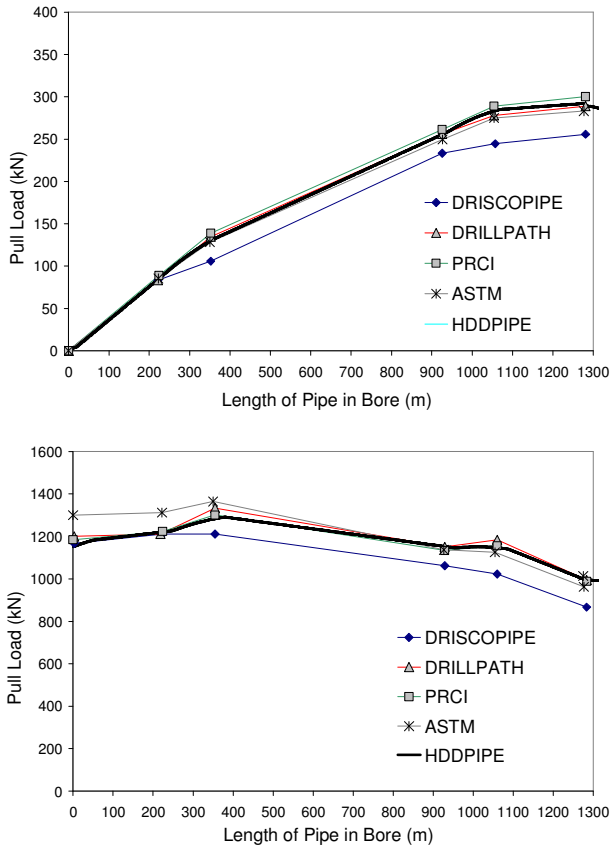

Figure 7. Pulling load versus pulled length:
(a) Lower bound (b) Upper bound

A high density polyethylene pipe with 40 mm outer diameter and 10 mm thickness is to be installed underground using horizontal directional drilling. The following set of parameters defines the 200 m operation:

Borepath profile (referring to Figure 2):

L_1 = 60 m L_2 = 80 m L_3 = 60 m
$\beta_1 = -10^o$ $\beta_2 = 1^o$ $\beta_3 = 12^o$
R_1 = 80 m R_{12} = 90 m R_{23} = 85 m
$\beta_o = 2^o$ Borehole Diameter = 700 mm

Pipe-soil interaction:

$\mu_{surface}$ = 0.3 μ_{bore} = 0.4
K = 1 MN/m per 1 m of borehole length
Drilling mud:
γ_{mud} = 14 kN/m^3 Q = 25 L/s μ = 0.1 pa.s

Head movement:
TP = 20 s TR = 15 s PL = 8.8 m

The viscoplastic constitutive model developed for HDPE by Zhang and Moore (1997) is used to model the mechanical response of the pipe during installation.

Figure 8 shows the pulling stress history at the pipe head during installation. Looking at the general trend, it can be noticed that the pulling stress increases as more pipe is pulled into the borehole. The rate of increase in the stress is not constant and a different slope in the stress history results when the pipe reaches a new region (a curve or a linear segment). Towards the end of each cycle, a drop in stress during rest times can be observed

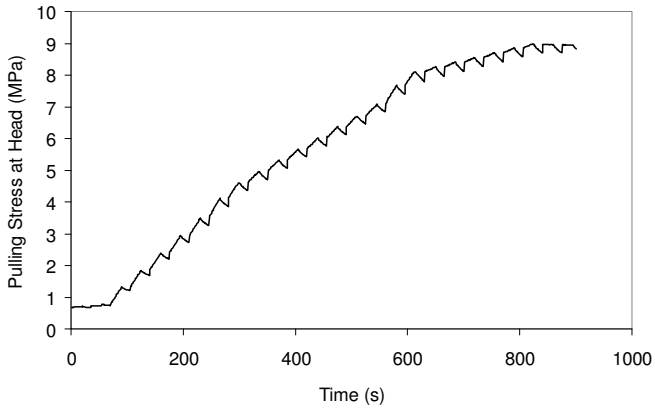

Figure 8. Pulling stress history at the pipe head.

The change of pipe stresses during the 20th pulling cycle is analyzed to further investigate the cyclic loading that occurs during the pulling force history. The reduction of the stress at the pipe head is clearly observed during the 15 s rest period between 685 s and 700 s, as shown in Figure 9.

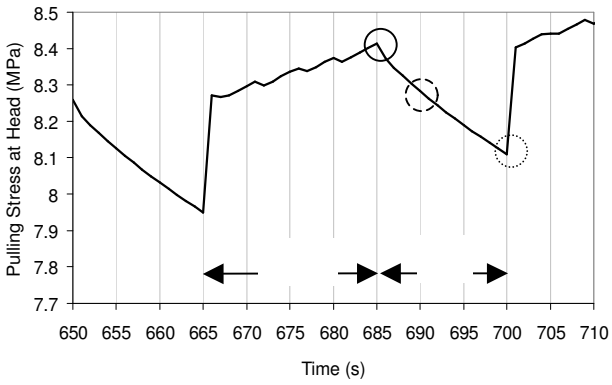

Figure 9. Pipe head stress during the 20th pulling cycle.

This reduction no only occurs near the pipe head but, to a lesser extent, along the entire pipe as Figure 10 demonstrates. This occurs because of relaxation of the elements that are restrained by the soil from creeping. The level of axial stress drop depends on several factors including the stress level achieved, the pipe material behaviour, the soil stiffness, and time at rest.

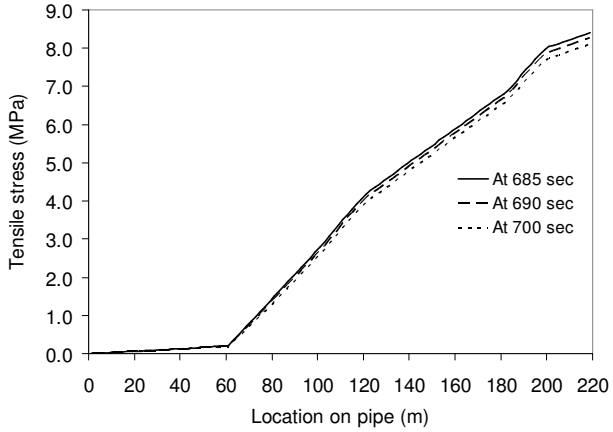

Figure 10. Change of stress along the pipe during the rest period after the 20th pulling cycle.

When the head recommences moving during a load cycle, the pipe recovers the load lost during the rest period (Figure 9). After that prompt stress increase, further change depends on pipe-borehole interaction.

6. CONCLUSION

A new model was developed to calculate tensile force and stress over the pipe length at any given time, knowing the history of pipe movement during installation. Gravity forces, pipe-soil interaction forces, and viscous drag force due to mud flow past the pipe are considered. Pipe-soil interaction is included, employing a simple model accounting for adhesion, friction, and soil stiffness. Model performance was successfully evaluated through comparisons to predictions from established methods. A further example problem demonstrated that the model provides details of cyclic loading history accounting for nonlinear, time dependent polymer behaviour. Development and use of this model is part of a comprehensive research program to calculate the short and long term behaviour of high density polyethylene pipes during and after HDD installations.

ACKNOWLEDGEMENT

This work is part of a Strategic Research project funded by the Natural Sciences and Engineering Research Council of Canada. Dr Moore's position at Queen's University is supported by the Canada Research Chairs program.

REFERENCES

ASTM International, Designation: F 1962 – 99, Standard guide for use of maxi-horizontal directional drilling for placement polyethylene pipe or conduit under obstacles, including river crossings, 1-17

Baumert, M.E. and Allouche, E.N. 2002. Methods for estimating pipe pullback loads for horizontal directional drilling (HDD) crossings, *Journal of Infrastructure Systems*, ASCE, 8(1): 12-19.

Baumert, M.E., Allouche, E.N., and Moore I.D. 2004. Experimental investigation of pull loads and borehole pressures during horizontal directional drilling installations, *Canadian Geotechnical Journal*, ASCE, 41: 672-685.

Dareing, D.W. and Ahlers, C.A. 1991. Tubular bending and pull-out forces in high curvature well bores, *Journal of Energy Recourses Technology*, 113: 133-139.

Drillpath™, 1996. Theory and user's manual, Infrasoft L. L. C., Houston, Texas, USA.

Driscopipe® 1993. Technical expertise application of driscopipe® in directional drilling and river-crossings, *Technical Note #*: 41.

Huey, D.P., Hair, J.D. and McLeod K.B. 1996. Installation loading and stress analysis involved with pipelines installed in horizontal directional drilling, *Proceedings of the No-Dig Conference – New Orleans, North American Society for Trenchless Technology*.

Haciislamoglu, M. and Langlinais, J. 1990. Non-Newtonian flow in eccentric annuli, *Journal of Energy Ressources Technology*, 112(3): 163-169.

Polak, M.A. and Lasheen, A. 2002. Mechanical modelling for pipes in horizontal directional drilling, *Tunneling and Underground Space Technology*, 16(1): S47-S55.

Zhang, C. and Moore, I.D. 1997. Nonlinear mechanical response of high density polyethylene. Part II: Uniaxial constitutive modeling, *Polymer Engineering and Science*, 37(2): 414-420.